Articles

High-Resolution NMR and Computer Modeling Studies of the Cannabimimetic Aminoalkylindole Prototype WIN-55212-2

Xiang-Qun Xie,*[,†,‡] Xiu-Wen Han,[†,||] Jian-Zhong Chen,[†] Michael Eissenstat,[▽] and Alexandros Makriyannis[†,‡,§]

Institute of Materials Science, Department of Pharmaceutical Sciences, School of Pharmacy, and Department of Molecular & Cell Biology, University of Connecticut, Storrs, Connecticut 06269, and Structural Biochemistry Program, SAIC, NCI−FCRDC, Frederick, Maryland 21702

Received October 19, 1998

Aminoalkylindoles (AAIs), although structurally dissimilar from the classical cannabinoids (CCs), are known to be capable of binding to cannabinoid receptors and of evoking cannabimimetic responses. However, their mode of binding remains unknown. In this communication, we have carried out further studies on the AAI prototype (*R*)-[2,3-dihydro-5-methyl-3-[(4-morpholinyl)methyl]pyrrolo[1,2,3-*de*]-1,4-benzoxazin-6-yl](1-naphthalenyl)methanone (WIN-55212-2, **1**) by the combined use of high-resolution 2D NMR and computer modeling. Our results suggest that the minimum energy conformations of the molecule **1** have distinct pharmacophoric features: (i) The naphthyl ring is oriented off the plane of the benzoxazine ring by approximately 59° with the carbonyl C═O group pointing toward the C2−CH_3 group. (ii) At the C10-position the axial morpholinomethyl conformation is preferred over the equatorial in order to relieve a steric interaction with the C2-methyl group. The preferred conformer as defined by the three key pharmacophores, naphthyl, morpholino, and 3-keto groups, shows that the morpholinyl ring of the molecule **1** deviates from the plane of the benzoxazine ring by about 32° and orients in the left molecular quadrant. This model supports the hypothesis that a certain deviation of the morpholino group from the plane of the indole ring in compound **1** is essential for cannabimimetic activity. We postulate that such an alignment by the respective pharmacophores allows them to interact optimally with the receptor. The results should help us to better understand the pharmacophoric requirements of the AAIs and serve as a basis for future SAR studies and drug design.

Introduction

Aminoalkylindole analogues (AAIs) were originally synthesized as cyclooxygenase inhibitors.[1,2] They were also found to possess antinociceptive activity, but unlike the opioids, such activity was not blocked by naloxone.[1,3] Additional evidence showed that AAI analogues lacking the cyclooxygenase inhibitory effect are also capable of binding to the cannabinoid receptor and of evoking a cannabimimetic response.[1−5] Therefore, AAIs represent a new class of cannabinoid receptor agonists. One of the most potent AAIs is **1**[1,5,6] (WIN-55212-2 in Figure 1), a compound which has received extensive attention because of its important role in the identification and characterization of the cannabinoid receptors. The most potent AAI analogues share three common features: (a) an indole ring system; (b) a tertiary amine moiety; and (c) a naphthoyl group. Several investigators[7−11] have explored pharmacophoric requirements for the AAIs.

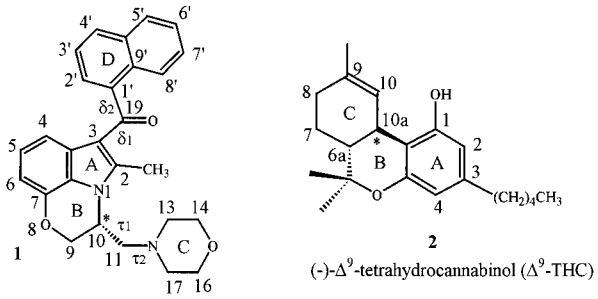

Figure 1. Structures of WIN-55212-2 (**1**) and (−)Δ^9-THC (**2**). In the molecule **1**, the C2−C3−C19−C1′, C3−C19−C1′-C9′, N1−C10−C11−N12, and C10−C11−N12−C13 dihedral angles correspond to $\delta 1$, $\delta 2$, $\tau 1$, and $\tau 2$, respectively.

These pharmacophoric AAI features were also correlated with those of the classical cannabinoids (CCs) (e.g., (−)-Δ^9-tetrahydrocannabinol (Δ^9-THC), **2** in Figure 1) which include a phenolic moiety, a tricyclic terpene system, and a hydrophobic side chain.[12] Such an exploration of the structural similarities and dissimilarities between the above two classes of cannabimimetic agents provides an opportunity for a better understanding of the molecular features required for cannabinoid activity. However, recent mutagenesis studies showed that the mutation of Lys^{192} (lysine) to Ala^{192} (alanine) in the CB1 receptor eliminated the binding affinity of the molecule

* To whom inquiries should be directed: U-136, IMS, University of Connecticut, Storrs, CT 06269. Tel: (860)-486-2922. E-mail: xie@uconnvm.uconn.edu.
† Institute of Materials Science.
‡ Department of Pharmaceutical Sciences.
§ Department of Molecular & Cell Biology.
▽ NCI−FCRDC.
|| Visiting scientist from Dalian Institute of Chemical Physics, Chinese Academy of Sciences, Dalian (116023), P.R.C.

10.1021/jm980592k CCC: $18.00
Published on Web 09/21/1999

2 and other ligands, but not the molecule **1**.[13,14] These data suggest that the molecules **1** and **2** may not bind at the same sites on the cannabinoid receptor or, alternatively, these two ligands may interact with the same site but with different binding orientations.

Because of its high affinity for the cannabinoid receptors and its potent activity as an agonist, the molecule **1** encodes important structural information regarding the activation of these receptors. In an effort to understand the receptor binding features of the AAI analogues, we have sought to determine the conformation of the molecule **1** in solution. Such information will be used in future ligand−receptor docking and CoMFA studies by computer modeling aimed at defining a pharmacophoric model for the AAIs.

In the present manuscript, we have examined the conformational properties of the molecule **1** in order to define, within this important ligand, those stereoelectronic features most probably associated with cannabimimetic activity and receptor binding. To accomplish our goal, we have combined high-resolution 2D NMR and computer modeling techniques and focused on: (i) the favored conformation of the morpholino group (C-ring); (ii) the preferred orientation of the naphthoyl group; and (iii) the relative position of the naphthyl ring (D-ring) with respect to the plane of the benzoxazine moiety (AB-ring). The ^{1}H and ^{13}C chemical shifts in the molecule **1** spectra were assigned by using 2D phase-sensitive DQF−COSY and ^{1}H−^{13}C HMQC. The preferred conformations were then determined by maximum agreement of the NOESY NMR data and computer-assisted conformational searches. Our studies show that in its preferred conformation the molecule **1** assumes an orientation in which the two polar pharmacophores, namely the morpholino and keto groups, are aligned on the same side of the molecule while the hydrophobic naphthyl group is oriented toward the opposite side. The model also suggests that a certain deviation of the 1-morpholino group from the plane of the indole ring is essential for cannabimimetic activity.

Experimental Section

Materials. The compound **1** was provided to us by Stering Winthrop Inc. Deuterated chloroform ($CDCl_3$) and tetramethylsilane (TMS) were purchased from Aldrich Chemical Co. (Milwakee, WI). NMR sample was prepared as a 0.02 M solution in deuterated chloroform ($CDCl_3$; Aldrich Chemical Co.), thoroughly degassed by the freeze−thaw method and sealed in high quality 5-mm NMR tubes. TMS was used as an internal chemical shift reference.

NMR Spectra. High-resolution ^{1}H NMR spectra were collected on a Bruker AVANCE DMX500 spectrometer with a 5-mm inverse detection triple resonance gradient probe and a BVT-2000 temperature controller. 2D phase-sensitive ^{1}H−^{1}H COSY spectra[15] (DQF−COSY) were recorded with a recycling delay of 2 s at a temperature of 298 K. The data sizes were 512w in F_1 and 2k in F_2 and were zero-filled in F_1 prior to 2D Fourier transformation to yield a 2k × 2k data matrix. The spectra were processed using a Qsine-bell window function in F_1 and F_2. 2D ^{1}H−^{1}H phase-sensitive NOESY[16] spectra were obtained using the acquisition parameters similar to the DQF−COSY with the addition of an 800-ms mixing time. A similar NOE pattern was observed in a NOESY experiment with a mixing time of 200 ms; however, the NOE cross-peaks were of lower intensity. 2D ^{1}H−^{13}C inverse correlated experiments with heteronuclear multiple quantum coherence (HMQC)[17] were performed using an inverse detection probe with a delay time of 3.57 ms for the J_{C-H} value and a delay of 0.35 s for bilinear rotation decoupling (BIRD) inversion pulse. 2D ^{1}H−^{13}C inverse correlated experiments with heteronuclear multiple bond correlation (HMBC)[18] were conducted using similar acquisition parameters as for HMQC, while choosing a proper delay time (50 ms) to enhance the observation of selected long-range couplings (e.g., $^2J_{C-H}$, $^3J_{C-H}$, and $^4J_{C-H}$).

Computer Molecular Modeling. Molecular modeling was carried out using the TRIPOS Sybyl molecular modeling package[19] with the Tripos empirical force field, on an SGI Octane R10000 workstation. Molecular mechanics and dynamics were utilized to examine the motions of atoms and to sample various minimum molecular conformations. The starting structure of the molecule **1** was built using standard bond lengths and angles from the Sybyl molecular modeling package and was further minimized. Molecular dynamics simulations[20] were performed using Tripos force field at 1000 K and time steps of 1 fs to search through the various conformations visited during the dynamics simulation. The detailed method has been reported elsewhere[21] and is briefly described here: (1) minimize the initial structure to relieve any overly strained coordinates using a quick minimization method (100 cycles and maximum derivative of 0.1 kcal mol^{-1} Å^{-1}); (2) perform molecular dynamics sampling of conformational space at a temperature of 1000 K by using the time steps of 1 fs, and simulate at this temperature for 300 ps with atomic coordinate trajectories recorded every 1 ps; (3) retrieve the 300 frames recorded during the dynamics run and minimize them using the steepest descent method followed by the conjugate gradient method until the maximum derivative is less than 0.001 kcal mol^{-1} Å^{-1}. Bond rotational energy barriers were carried out by using MOPAC/AM1,[22] with intervals of 10° for bond rotation as reported elsewhere.[23]

Results

NMR Spectral Assignments. The ^{1}H and ^{13}C spectral assignments of the molecule **1** were made on the basis of the coupling connectivities in the ^{1}H−^{1}H DQF−COSY spectrum (Figure 2) and ^{1}H−^{13}C HMQC spectrum (not shown). Assignments for the benzoxazine (AB-ring) and naphthyl (D-ring) ring protons were made on the basis of integration, chemical shifts, and analysis of the expanded regional contour plots of the phase-sensitive DQF−COSY and HMQC spectra. A logical starting point is the H-2′ of the naphthyl ring that can be readily identified in the 2D ^{1}H−^{13}C HMBC spectrum (Figure 2 insert), showing a cross-peak at 7.57 and 190.4 ppm attributed to the long-range ^3J-coupling of H-2′ and C═O. Having assigned the H-2′, we can then find its connections with H-3′ (7.52 ppm) and H-4′ (7.99 ppm) in the DQF−COSY spectrum (Figure 2). Similarly, we assigned the C1′ at 140.2 ppm by identifying the $^3J_{H3'-C1'}$ coupling and the H-8′ at 8.08 ppm by the $^3J_{C1'-H8'}$ in the 2D ^{1}H−^{13}C HMBC spectrum. We can continue from H-8′ to deduce the H-7′, H-6′, and H-5′ on the basis of their connectivities in the 2D DQF−COSY spectrum. By the same analogy, we were able to assign all protons and carbons on the AB- and D-rings. The upfield region assignments are less complicated and can be determined on the basis of their chemical environments and peak integrations. Chemical shifts were further confirmed by comparing the DQF−COSY, HMQC, and HMBC spectra. The complete assignments of proton and carbon chemical shifts for the molecule **1** are summarized in Table 1.

NOEs−Dipolar Interactions. The nuclear Overhauser effect (NOE) is one of the most important NMR parameters used in conformational analysis since the magnitude of the NOE is inversely proportional to the sixth power of the interproton distance in space (I_{NOE}

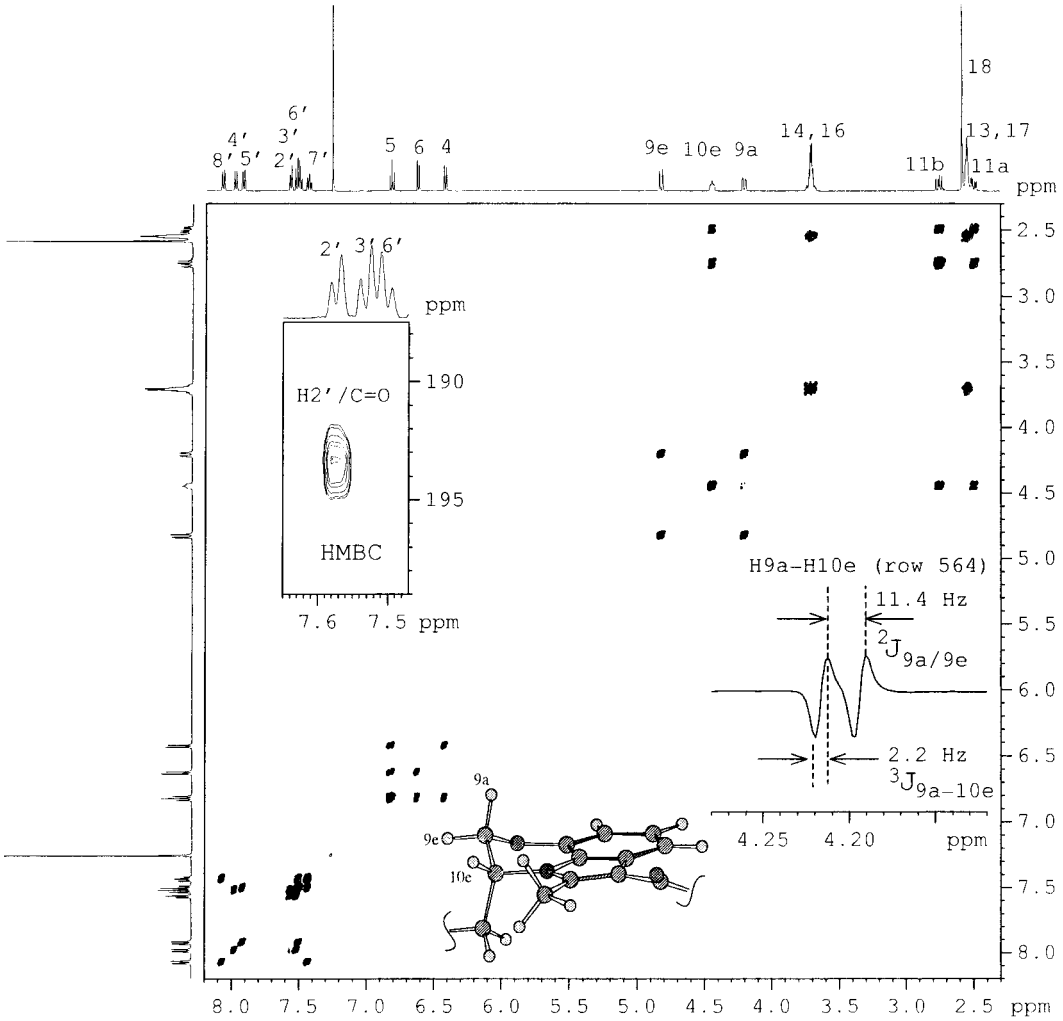

Figure 2. 500-MHz 2D $^1H-^1H$ DQF−COSY spectrum of the molecule **1** in $CDCl_3$ solution at 298 K. A cross section parallel to the F_2 dimension (row 564) was sliced out through the H-10e resonance in the COSY spectrum, showing couplings between H-9a/H-10e (2.2 Hz) and H-9a/H-9e (11.4 Hz). Inset: An expanded region of the 2D $^1H-^{13}C$ 2D HMBC spectrum showing the H-2′ and C═O connectivity as a logical starting point for chemical shift assignments.

$\propto r^{-6}$). Typically, an observed NOE cross-peak indicates that the two protons are within a distance of 3.0 Å and exhibit through-space coupling with each other. Beyond the 3.0 Å range, the NOE is weak, and the effect becomes barely detectable at 4.5 Å.[16] To obtain the NOE values for the molecule 1, the 2D $^1H-^1H$ phase-sensitive NOESY spectrum was obtained (Figure 3). Our data show a strong NOE cross-peak between the D-ring H-2′ (7.57 ppm) and the aromatic AB-ring H-4 (6.42 ppm), indicating that these two protons are spatially near and coupled through a dipole−dipole interaction. This also defined the relative orientation of the D-ring with respect to the AB-ring as will be discussed later. Such a conformation also explains the upfield shift of the H-4 proton since H-4 is located at the top of the aromatic ring and thus is partially shielded. Additional NOEs were observed between H-10e and $-CH_3$; H-2′ and $-CH_3$; H-8′ and $-CH_3$; H-10e and H-13,17; H-9e and H-13,17; as well as H-9e and H-11 protons as shown in Figure 3. The above NOE cross-peaks provide important information regarding the preferred orientation of the D- and C-rings with respect to the AB-ring, as detailed later.

Computer Modeling. Molecular dynamics/mechanics simulations were carried out to search for the

Table 1. ^1H NMR (500 MHz) and ^{13}C NMR (125 MHz) Chemical Shift Assignments for the molecule **1**

hydrogen and carbon	^1H (δ, ppm)	^{13}C (δ, ppm)
2		143.8
3		115.6
3a		127.1
4	6.42 (d, 7.8 Hz)	114.0
5	6.83 (t, 7.8 Hz)	122.8
6	6.63 (d, 7.8 Hz)	106.4
7		142.3
7a		123.6
9e	4.84 (d, 11.7 Hz)	66.5
9a	4.21 (d, 11.7 Hz)	66.5
10e	4.46 (br)	50.2
11a	2.46 (dd, 12.7, 5.4 Hz)	59.1
11b	2.76 (dd, 12.7, 8.8 Hz)	59.1
13,17	2.56 (br)	54.2
14,16	3.72 (br)	66.9
18	2.59 (s)	12.1
1′		140.2
2′	7.57 (d, 7.8 Hz)	125.3
3′	7.52 (t, 7.8 Hz)	125.0
4′	7.99 (d, 7.8 Hz)	129.9
5′	7.93 (d, 7.8 Hz)	128.2
6′	7.51 (t, 7.8 Hz)	126.2
7′	7.44 (t, 7.8 Hz)	126.8
8′	8.08 (d, 7.8 Hz)	125.5
9′		130.2
10′		133.7
C═O		190.4

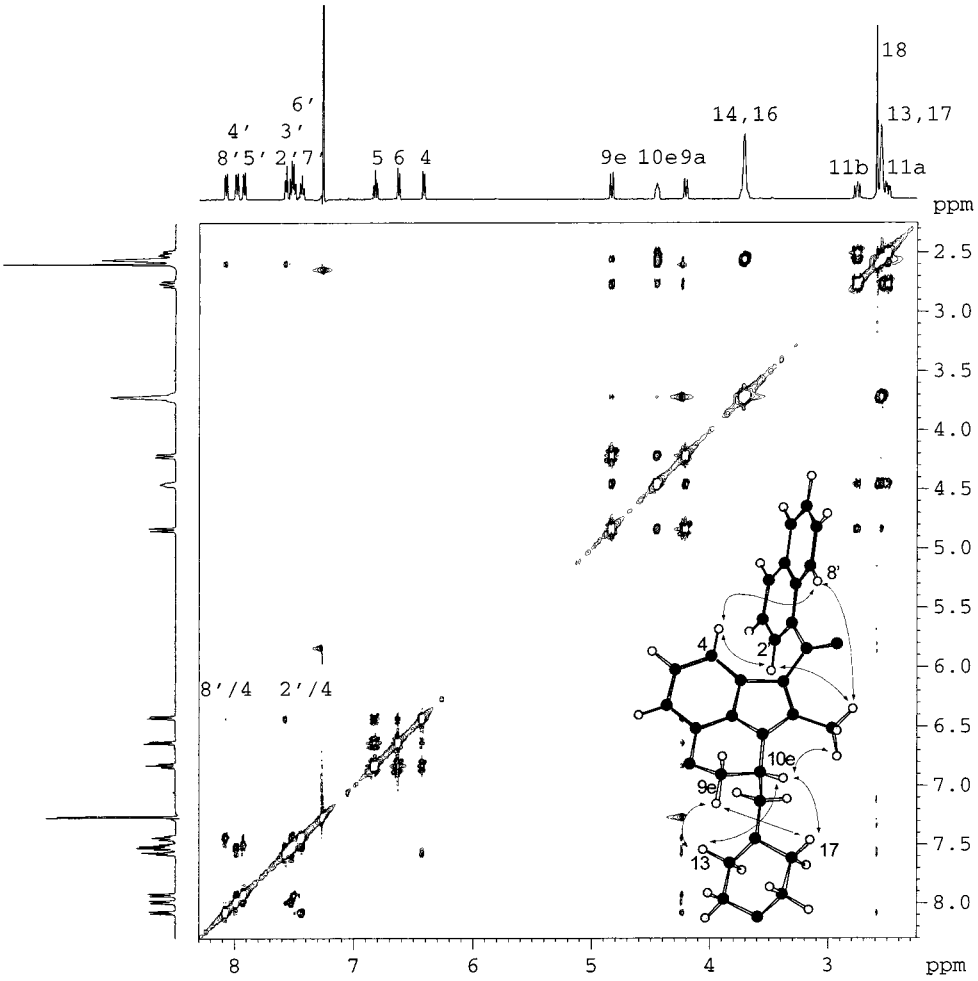

Figure 3. 500-MHz 2D $^1H-^1H$ NOESY spectra of the molecule **1** in $CDCl_3$ solution at 298 K. The NOE dipolar interactions for WIN-55212-2 are indicated with arrows.

preferred and low-energy conformations of the molecule **1**. Dynamics motions were simulated at a high temperature (1000 K) to increase the probability of inducing conformational transitions past any possible high-energy barriers. A total of 300 000 conformations or frames (1-fs intervals) were sampled during the simulation. Molecular mechanics energy minimizations were carried out for each of the 300 conformers. This operation resulted in a convergence of these conformers into several families. As depicted in Figure 4, they represent six families of minimum energy conformations extracted from 300 frames of conformers which were sampled during the dynamics simulation and followed by energy minimization. The calculated dihedral angles and relative conformational energies are summarized in Table 2. The energy difference between these six conformers is less than 1 kcal/mol. As confirmatory evidence for the above results, we have also carried out NOE-constrained dynamics simulation as we have described elsewhere.[21] Indeed, the two minimum energy conformers obtained using this approach were identical with conformers V and VI described above. As shown in Figure 4, the two dihedral angles ($\delta 1$ and $\delta 2$) between the D- and AB-rings tend to be localized around $\pm 150°$ and $\pm 40°$, respectively, while the $\tau 1$ and $\tau 2$ angles between the C- and AB-rings have two possible values, namely, $\pm 177°$ or 55° and 135° or $-95°$, respectively. The rotational barriers for $\delta 1$, $\delta 2$, $\tau 1$, and $\tau 2$ were calculated using MOPAC/AM1 and found to be 7.44, 7.69, 4.97, and 5.31 kcal/mol, respectively. Our results show that conformer I is the lowest-energy conformer, while the other five conformers have higher energies by approximately 0.2−1.1 kcal/mol. Among these, conformer V which exhibits maximum agreement with the experimentally determined NOE data has the oxygen atom of the carbonyl group pointing toward the C2-methyl group, and the O−C19−C3−C2 dihedral angle being *syn* and equal to −28°. In this conformation, the D-ring deviates from the plane of the AB-ring by 59°, and the $\delta 1$ and $\delta 2$ dihedral angles are 152° and 138°, respectively. The energy difference between conformers V and I is small, approximately 1.1 kcal/mol.

Discussion

Our conformational analysis of the molecule **1** combines the experimental results determined by solution NMR experiments with computational data obtained from molecular mechanics/dynamics calculations. The approach involves analyzing the conformational properties of individual molecular components and subsequently combining them to provide a complete picture of the molecule under study. The preferred conformation as defined by the alignment of the pharmacophoric groups is thus determined by maximal agreement between the experimental and computational results.

Orientation of the D- and AB-Rings. The ^1H NMR

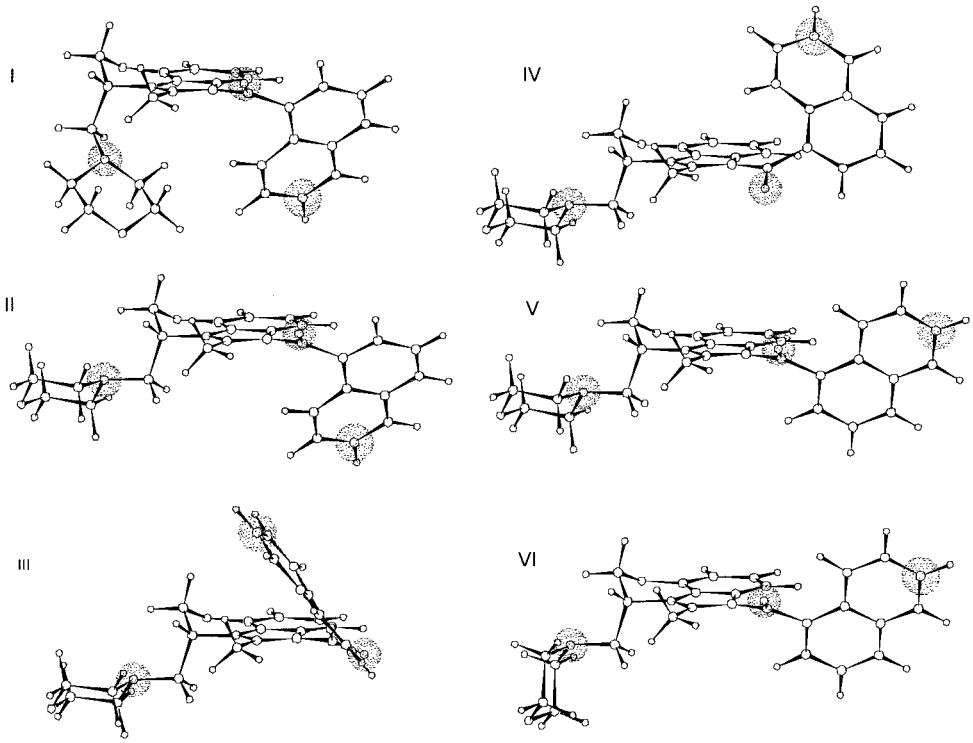

Figure 4. Molecular graphic representation of six energetically favored conformations for the molecule **1** obtained from energy minimization of structures occurring along the molecular dynamics trajectory.

Table 2. Summary of the Structural Features and Relative Energies for the Preferred Conformers of the Molecule **1** Based on Energy Minimizations Followed by Dynamics Simulations at 2500 K for 300 ps

frame no.	relative energy (kcal/mol)	$\delta 1$	$\delta 2$	$\tau 1$	$\tau 2$	H-2′/H-4 (Å)	H-8′/H-4 (Å)
I	19.56	155°	−41°	54°	−102°	4.12	3.67
II	19.61	152°	−37°	−178°	137°	4.26	3.68
III	19.63	−29°	−38°	176°	−95°	5.32	4.10
IV	19.84	−153°	37°	−178°	−91°	4.16	3.67
V	20.51	152°	138°	−178°	137°	3.02	4.14
VI	20.62	151°	138°	178°	132°	3.02	4.14

NOESY spectrum of the molecule **1** shows a relatively strong NOE cross-peak between the H-4 of AB-ring and the H-2′ of D-ring, indicating their close spatial proximity, and only a very weak one between H-8′ and H-4. The NOE result is congruent with the molecular structure of the molecule **1** depicted in Figure 3. Such a conformation also explains the observed upfield shift of the H-4 proton which faces the center of the aromatic D-ring and is shielded by it. The results are consistent with previously reported data for pravadoline and its analogues using NMR and X-ray.[1] Of the six low-energy conformers identified from our computational studies shown in Figure 4, conformers I, II, III, and IV show interproton distances between H-2′ and H-4 (∼4.2 Å) larger than those between H-8′ and H-4 (∼3.6 Å) and are therefore not congruent with the NMR results. Conversely, conformers V and VI have the oxygen atom of the carbonyl group pointing toward the C2-methyl group with the dihedral angle (O−C19−C3−C2) of −28° and the D-ring deviating from the plane of the A-ring by about 59° ($\delta 1 = 152°$, $\delta 2 = 138°$), which are congruent with our 2D NOESY NMR experimental data.

Conformation of the B- and C-Rings. The conformation of the benzoxazine group was analyzed by examining the vicinal and geminal coupling constants for the B-ring. These were extracted from a 1D ^{1}H spectrum with resolution enhancement techniques and confirmed by slicing out the cross section plot of the 2D DQF−COSY spectrum along the F_2 dimension (Figure 2). The measured coupling constants $^3J = 2.21$ and 11.4 Hz correspond to the coupled spin pairs of H-9a/H-10e and H-9a/H-9e, respectively, which revealed a preferred partial chair conformation for the B-ring with the N1−C7a−C7−O8 atoms being coplanar as shown in the insert of Figure 2. The observed NOE cross-peak between H-10e (4.46 ppm) and CH_3 (2.59 ppm) also confirmed a B-ring conformation (Figure 3) in which the morpholinomethyl substituent is axial. NOE cross-peaks were also observed between H-9e (4.84 ppm) and H-11 (2.56, 2.76 ppm) protons, as well as between H-9e (4.84 ppm) and H-13,17 (2.56 ppm) protons, and are congruent with conformers II, III, IV, and V.

The preferred conformations of the morpholinyl substituent as determined by computer molecular modeling are shown in Figure 4 with the preferred dihedral angles between the AB- and C-rings $\tau 1 = 177°$ or 55° and $\tau 2 = +135°$ or −90°. Among the low-energy conformers $\tau 1$ appears to be localized at 177°, a preference which may be attributed to the relative high rotational energy barrier around that bond. Conformer I in which the morpholinyl group is *syn* can be ruled out because the calculated distances between H-9e and H-13 or H-17 are over 5 Å and therefore not consistent with the NOE results. All of the remaining conformers exhibit a

similar *anti* orientation for the morpholinyl substituent except that in conformer VI the N-substituent of the C-ring is axial unlike the other conformers where it is equatorial. As discussed above, the calculated D-ring conformations for the conformers II, III, and IV are also inconsistent with the NMR NOESY results. Therefore, only conformers V and VI are congruent with the experimentally observed NOE data, according to which the interproton distances for H-2′/H-4, H-8′/H-4, and H-9e/H-13,17 are 3.01, 4.14, and 3.13 Å, respectively. The ^{1}H NMR frequencies due to the morpholino group consist of two broad multiplets, one corresponding to the 14-CH_2 and 16-CH_2 protons at 3.72 ppm and the other to the 13-CH_2 and 17-CH_2 protons at 2.56 ppm. The nearly degenerate chemical shifts of the axial and equatorial protons on the C-ring suggest that the ring is undergoing a rapid conformational exchange in solution. The conformational exchange between these protons is also suggested by the results of a variable temperature study, in which the multiplets of the C-ring protons were observed to coalesce at a lower temperature (263 K) (results not shown). Our combined NMR and computational data are congruent with both conformers V and VI. However, the presence of a relatively strong NOE between H-9e and H-13,17 and a very weak NOE between H-9e and H-14,16 may indicate that of the two, the conformer V is preferred in solution and has closest agreement with the NMR results.

Pharmacophore Alignment. As described above, the preferred low-energy conformations of the cannabimimetic AAI prototype **1** have certain distinctive features: (i) The orientation of the D-ring deviates from the plane of the AB-ring by approximately 59° with the carbonyl C═O group pointing toward the C2-methyl group. (ii) The C10-R, a morpholinomethyl substituent, prefers an axial orientation over an equatorial one in order to relieve a steric interaction with the C2-methyl group. (iii) In its preferred orientation, the morpholinyl substituent has its plane off the AB-ring with the dihedral angles $\tau 1 = 178°$ and $\tau 2 = 132°$, respectively.

Figure 5 shows a graphical representation of the preferred conformer of the molecule **1** with the three key pharmacophores, the naphthyl, morpholino, and 3-keto groups, aligned in a manner which allows all of the polar groups to be pointing toward one side of the molecule. In such an alignment the C-ring of the molecule **1** deviates from the plane of the AB-ring by approximately 32° and orients into the left molecular quadrant. This is reminiscent with earlier work published by Makriyannis[12,23,24] and Reggio[25] in which it was suggested that differences in cannabinoid potencies among the tricyclic classical cannabinoids could be explained by the deviation from planarity of the C-ring and its relative orientation with regard to the plane of the aromatic Ph-OH. Such an example is shown in Figure 5 in which the biologically active molecule 2 has its C-ring deviating from planarity by about 20° with regard to the plane of the phenol ring.

Fragmentary data from biochemical studies involving single-site receptor mutations suggest that the CCs and the AAIs represented by the molecules **1** and **2**, respectively, do not share identical binding modes at the CB1 receptor. However, our results argue that, notwithstanding the above data, the two groups of cannabimimetic ligands share some common pharmacophoric features and are also oriented in a similar manner within the cell membrane where these ligands are favored to partition.[21] Within the CCs, the phenolic hydroxyl and the hydrophobic side chain which are attached to a rigid tricyclic template are two key pharmacophores involved in the binding to CB1. Additionally, early results had shown that within the amphipathic membrane bilayer cannabinoids orient with their tricyclic ring system perpendicular to the phospholipid chains while the polar phenolic OH and the hydrophobic tail interact with the polar and hydrophobic membrane components, respectively.[26] We have argued[21] that such an orientation is optimal for a productive ligand−receptor interaction through fast lateral diffusion within the bilayer. By analogy, within the molecule **1** structure, the polar carbonyl and hydrophobic naphthyl groups attached to an indole template serve as key pharmacophoric elements involved in the interaction with the CB1 receptors. Within the membrane, the above two pharmacophores are expected to orient toward the bilayer's polar and hydrophobic components, respectively.

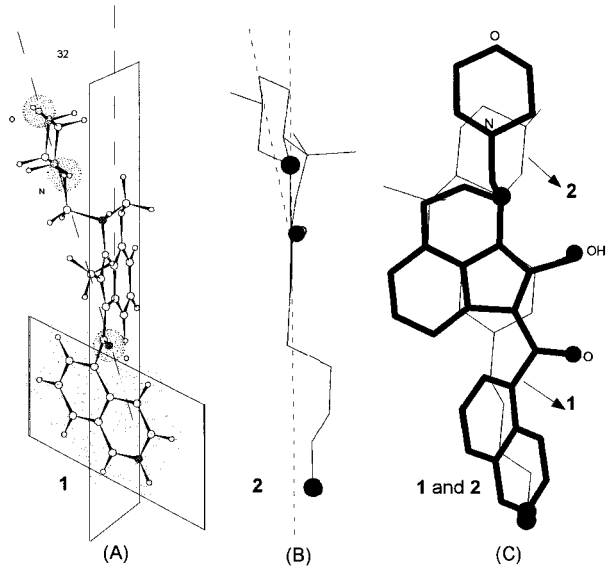

Figure 5. (A) Graphical representation of the favored conformations of the molecule **1**, in which the atoms highlighted with van der Waals electron surfaces are potential hydrogen-bonding centers, while the aromatic rings constitute the hydrophobic components. (B) Conformation of the molecule **2** from X-ray crystallographic data.

Thus, both CCs and AAIs are amphipathic molecules possessing hydrophobic and polar groups anchored on a rigid template. The proper relative alignment of the polar groups with regard to the hydrophobic components in each molecule may be an important determinant of their ability to interact productively with the receptor site.[12] The phenolic OH of the molecule **2** and the corresponding carbonyl group of the molecule **1** (Figure 5) are pointing toward the same side of the molecule and are positioned for a potential H-bonding interaction with the receptor site.[26] The correct chirality appears necessary for a proper alignment of the pharmacophores.[24] When properly aligned, the biologically active AAIs and CCs respectively have their morpholinyl and cyclohexyl components in the same quadrant and attach themselves to the same CB1 active site, although this

interaction may involve different amino acid residues and different binding motifs. Such differences in binding motifs for the different cannabimimetic classes with the CB1 active site may explain the variations in binding affinities among these classes when CB1 mutants are used.[13,14] The pharmacophore model presented above requires further validation by testing against other AAI analogues; however, it may serve as a useful basis for future SAR work.

Conclusion

In this study, high-resolution NMR experiments have provided detailed information on the conformation of the AAI cannabimimetic ligand **1** in solution and allowed us to identify a preferred conformer. Additionally, molecular modeling studies confirmed that the preferred conformation in solution was indeed a low-energy conformer. The results obtained by a combination of these two techniques suggest a low-energy conformer in which the individual pharmacophores are suitably arranged so that the polar groups are pointing upward while hydrophobic components are oriented in the opposite direction. The discovery that certain AAIs possess potent cannabimimetic properties and high affinities for the cannabinoid receptor has expanded the spectrum of SARs and introduced additional molecular tools for studying the stereoelectronic requirements at the cannabimimetic sites. Currently, we are continuing our work with other AAI analogues. The defined conformation of the prototype AAI ligand will be used for more extensive studies using CoMFA and ligand docking studies and will be reported separately.

Acknowledgment. This work was supported by grants from the National Institutes of Health (DA11510). We acknowledge Pfizer Inc. for providing assistance with the molecular modeling package and Drs. J. B. Matthew and F. DiCapua for their help. We also thank Dr. William C. Curtiss at Tripos Inc. for his discussion regarding computer modeling methods.

References

(1) Bell, M. R.; D'Ambra, T. E.; Kumar, V.; Eissenstat, M. A.; Herrmann, J. L.; Wetzel, J. R. Jr.; Rosi, D.; Philion, R. E.; Daum, S. J.; Hlasta, D. J.; Kulling, R. K.; Ackerman, J. H.; Haubrich, D. R.; Luttinger, D. A.; Baizman, E. R.; Miller, M. S.; Ward, S. J. Antinociceptive (aminoalkyl) indoles. *J. Med. Chem.* **1991**, *34*, 1099−1100.

(2) Pacheco, M.; Childers, S. R.; Arnold, R.; Casinao, F.; Ward, S. J. Aminoalkylindoles: actions on specific G-protein-linked receptors. *J. Pharmacol. Exp. Ther.* **1991**, *257*, 170−183.

(3) Ward, S. J.; Mastriani, D.; Casino, F.; Arnold, R. Pravadoline: profile in isolated tissue preparations. *J. Pharmacol. Exp. Ther.* **1990**, *255*, 1230−1239.

(4) D'Ambra, T. E.; Estep, K. G.; Bell, M. R.; Eissenstat, M. A.; Josef, K. A.; Ward, S. J.; Haycock, D. A.; Baizman, E. R.; Casiano, F. M.; Beglin, N. C.; Chippari, S. M.; Grego, J. D.; Kullnig, R. K.; Daley, G. T. Conformationally restrained analogues of pravadoline: nanomolar potent, enantioselective, (Aminoaklyl) indole Agonists of the Cannabinoid Receptor. *J. Med. Chem.* **1992**, *35*, 124−135.

(5) Devane, W. A.; Dysarz III, F. A.; Johnson, M. R.; Melvin, L. S.; Howlett, A. C. Determination and characterization of a cannabinoid receptor in rat brain. *Mol. Pharmacol.* **1988**, *34*, 605−613.

(6) Hlasta, D. J.; Luttinger, D.; Perrone, M. H.; Silbernagel, M. J.; Ward, S. J. Alpha 2-adrenergic agonists/antagonists: the synthesis and structure−activity relationships of a series of indolin-2-yl and tetrahydroquinolin-2-yl imidazolines. *J. Med. Chem.* **1987**, *30*, 1555−1562.

(7) Huffman, J. W.; Dai, D.; Martin, B. R.; Compton, D. R. Design, synthesis and pharmacology of cannabinoid indoles. *Bioorg. Med. Chem. Lett.* **1994**, *4*, 563−56.

(8) Eissenstat, M. A.; Bell, M. R.; D'Ambra, T. E..; Estep, K.; Haycock, D. A.; Olefirowicz, E. M.; Ward, S. J. Aminoalkylindoles (AAIs): structurally novel cannabinoidminetics. *NIDA Res. Monogr. Ser. No. 105* **1991**, 427.

(9) Thomas, B. F.; Compton, D. R.; Martin, B. R.; Semus, S. F. Modeling the cannabinoid receptor: A three-dimensional quantitiative structure−activity analysis. *Mol. Pharmacol.* **1991**, *40*, 656−665.

(10) Reggio, P. H.; Basu-Dutt, S.; Hurst, D. P.; Patel, M. J.; Seltzman, H. H.; Thomas, B. F. What is the bioactive conformation of aminoalkylindoles at the CB1 receptor? insights gained from the E and Z naphthylidenes. International Cannabinoid Research Society, June 1997.

(11) Xie, X. Q.; Eissenstat, M. A.; Makriyannis, A. Common cannabimimetic pharmacophoric requirements between aminoalkyl indoles and classical cannabinoids. *Life Sci.* **1995**, *56*, 1963−1970.

(12) (a) Makriyannis, A.; Rapaka, R. S. The molecular basis of cannabinoid activity. *Life Sci.* **1990**, *47*, 2173−2184. (b) Makriyannis, A. The role of cell membranes in cannabinoid activity. In *The Cannabinoid Receptors*; Pertwee, R. G., Ed.; Academic Press: London, U.K., 1996; pp 87−116.

(13) Song, Z. H.; Bonner, T. I. A Lysine reside of the cannabinoid receptor is critical for receptor recoginition by several agonists but not WIN55212−2. *Mol. Pharmacol.* **1996**, *49*, 891−896.

(14) Shire, D.; Calandra, B.; Delphech, M.; Dumont, X.; Kaghad, M.; Le Fur, G.; Caput, D.; Ferrara, P. Structural Features of the Central Cannabinoid CB1 receptor involved in the binding of the specific CB1 antagonist SR141716A. *J. Biol. Chem.* **1996**, *271*, 6941−6946.

(15) Marion, D.; Wuthrich, K. Application of phase sensitive two-dimensional correlated spectroscopy (COSY) for measurements of $^1H-^1H$ spin−spin coupling constants in proteins. *Biochem. Biophys. Res. Commun.* **1983**, *113*, 967−974.

(16) Bodenhausen, G.; Kogler, H.; Ernst, R. R. Selection of coherence transfer pathways in NMR pulse experiments. *J. Magn. Reson.* **1984**, *58*, 370−388.

(17) Bax, A.; Subramanian, S. Sensitivity-enhanced 2D heteronuclear shift correlation NMR spectroscopy. *J. Magn. Reson.* **1986**, *67*, 565−569.

(18) Ruiz-Cabello, J.; Vuister, G. W.; Moonen, C. T. W.; Gelderen, P. V.; Cohen, J. S.; van Zijl, P. C. M. Gradient-enhanced heteronuclear correlation spectroscopy. *Theory Exp. Aspects* **1992**, *100*, 282−302.

(19) SYBYL (version 6.4) molecular modeling software packages from TRIPOS Associates, Inc., St. Louis, MO 63144.

(20) Hagler, A. T. Theoretical simulation of conformation, energetics, and dynamics of peptides. In *The Peptides*: Conformation in Biology and Drug Design; Udenfriend, S., Meienhofer, J., Eds.; Academic Press: New York, 1985; pp 214−300.

(21) Xie, X. Q.; Melvin, L. S.; Makriyannis, A. The Conformational Properties of the Highly Selective Cannabinoid Receptor Ligand CP-55,940. *J. Biol. Chem.* **1996**, *271*, 10640.

(22) Dewar, M. A.; Zoebisch, E. G.; Healy, E. F.; Stewart, J. P. AM1, A New General Purpose Quantum Mechanical Molecular Mode. *J. Am. Chem. Soc.* **1985**, *107*, 3902−3909.

(23) Xie, X. Q.; Yang, D. P.; Melvin, L. S.; Makriyannis, A. Conformational analysis of a prototype nonclassical cannabinoid CP-47,497 using 2D NMR and computer molecular modeling. *J. Med. Chem.* **1994**, *47*, 1418−1426.

(24) Kriwacki, R. W.; Makriyannis, A. The conformational analysis of Δ9- and Δ9,11-tetrahydrocannabinols in solution using high-resolution nuclear magnetic resonance spectroscopy. *Mol. Pharmacol.* **1989**, *35*, 495−503.

(25) Reggio, P. H.; Greer, K. V.; Cox, S. M. The importance of the orientation of the C9 substituent to cannabinoid activity. *J. Med. Chem.* **1989**, *32*, 1630−1635.

(26) Makriyannis, A. The role of the phenolic hydroxyl group during the tetrahydro-cannabinol:membrane interactions. In *Marijuana: An International Research Report*; Chesher, G., Consroe, P., Musty, R., Eds.; Australian Publishing Service: Canberra, 1988; pp 437−451.

JM980592K